Transiting Planets
Proceedings IAU Symposium No. 253, 2008
Frédéric Pont, Dimitar Sasselov & Matthews Holman, eds.

doi:10.1017/S1743921308026410

Emergent Exoplanet Flux: Review of the Spitzer Results

Drake Deming

Planetary Systems Laboratory
Code 693, NASA's Goddard Space Flight Center
Greenbelt MD 20771 USA
email: ddeming@pop600.gsfc.nasa.gov

Abstract. Observations using the *Spitzer Space Telescope* provided the first detections of photons from extrasolar planets. *Spitzer* observations are allowing us to infer the temperature structure, composition, and dynamics of exoplanet atmospheres. The Spitzer studies extend from many hot Jupiters to the hot Neptune orbiting GJ 436. Here I review the current status of *Spitzer* secondary eclipse observations, and summarize the results from the viewpoint of what is robust, what needs more work, and what the observations are telling us about the physical nature of exoplanet atmospheres.

1. Introduction

The powerful astrophysical leverage provided by transits enables us to study extrasolar planets directly, i.e., by detection of their emergent radiation. The *Spitzer Space Telescope* has provided the bulk of these detections. The first *Spitzer* measurements of exoplanet secondary eclipses were announced in 2005. Two independent groups (Charbonneau *et al.* 2005; Deming *et al.* 2005) measured eclipses for two different planets, using two different *Spitzer* instruments, and obtained very similar results (Figure 1).

Since each eclipse was independently measured to $\sim 6\sigma$ significance, exoplanet thermal emission was securely detected. The discovery of transits in HD 189733b (Bouchy *et al.* 2005) provided an opportunity to measure exoplanet thermal emission at higher signal-to-noise ratio. Initial observations of HD 189733b at 16 μm (Deming *et al.* 2006) showed an eclipse of the planet at 32σ significance (Figure 2), and subsequent work using the IRAC instrument has detetcted the planet's flux to 60σ precision at 8 μm (Knutson *et al.* 2007). This extraordinary level of precision in measuring exoplanet thermal emission allows many intersting studies that could hardly have been imagined when the first extrasolar planets were detected by radial velocity studies.

In this review I summarize highlights from *Spitzer* secondary eclipse measurements, with some discussion of transmission spectroscopy during transit. The quality of work in this field has been uniformly high, but I will summarize the results from the viewpoint of what is robust, and what I believe needs more work and clarification.

2. Spectral Energy Distributions from Photometry

The depth of a planetary eclipse measures the brightness of the planet at that wavelength, in units of the stellar brightness. Combining results from multiple eclipses at different wavelengths allows us to reconstruct the spectral energy distribution of the planet at photometric spectral resolution (typically, $\lambda/\delta\lambda \sim 3$). The results are usually shown in 'contrast' units, i.e., planet divided by star, since that is what we actually measure. The contrast amplitude of exoplanet eclipses is greatest at the longest wavelengths.

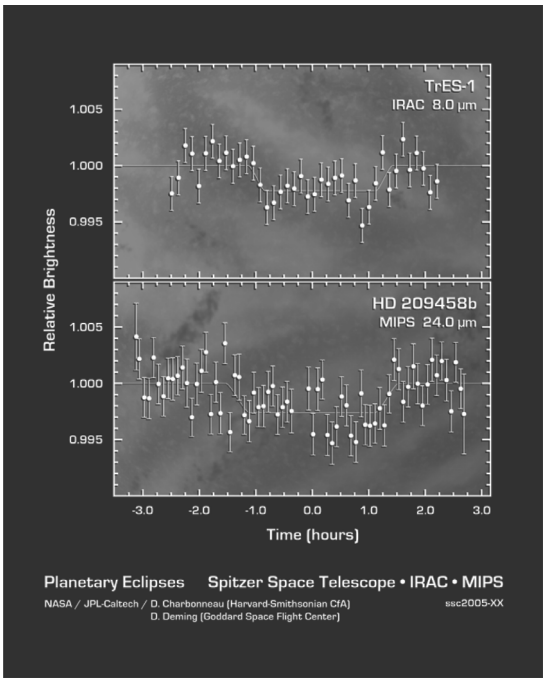

Figure 1. First detections of exoplanet thermal emission using the *Spitzer Space Telescope*. Plotted are the secondary eclipses of TrES-1 at 8 μm (top, Charbonneau *et al.* 2005), and HD 209458b at 24 μm (bottom, Deming *et al.* 2005)

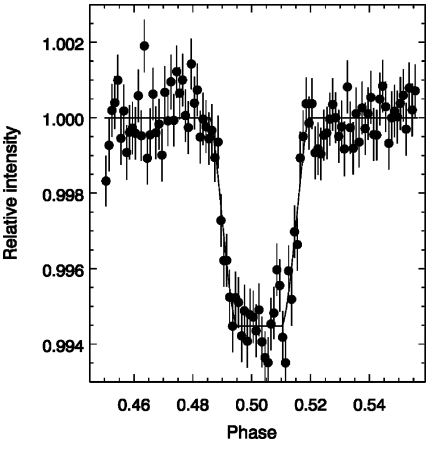

Figure 2. Eclipse of HD 189733b at 16 μm (Deming *et al.* 2006)

In the Rayleigh-Jeans limit, the eclipse amplitude (A_λ) is (Charbonneau 2003):

$$A_\lambda = \left(R_p^2/R_s^2\right)(T_p/T_s), \tag{2.1}$$

where (R_p^2/R_s^2) is the ratio of planet-to-star area, and (T_p/T_s) is the ratio of planet-to-star brightness temperature. Assuming that the planet and star resemble blackbodies (a reasonable approximation at the longest wavelengths), then:

$$T_p = \alpha T_s \theta^{1/2}, \tag{2.2}$$

https://doi.org/10.1017/S1743921308026410 Published online by Cambridge University Press

where θ is the angular diameter of the star as seen from the planet, and α is a constant that contains the planet's albedo, circulation properties, etc. An important corollary of Eqs. 2.1 and 2.2 is the effect of smaller parent stars (e.g., M-dwarfs). As we proceed down the main sequence, R_s and θ decrease, but the exponents imply that the (R_p^2/R_s^2) term dominates over $\theta^{1/2}$. Hence planets orbiting small stars will generally exhibit deeper eclipses, and their emergent flux will be more detectable for that reason. Moreover, the habitable zone moves closer to lower main sequence stars, and the transit probability increases inversely to the planet's orbit radius. This circumstance is a major impetus for finding terrestrial planets in the habitable zones of M-dwarfs (Charbonneau and Deming, 2007).

The time of the secondary eclipse is very sensitive to the eccentricity of the orbit, specifically to $e\cos\omega$ (Charbonneau 2003). For example, the eclipse of GJ 436b occurs at phase 0.585 ± 0.005 (Deming *et al.* 2007), more than five hours after the mid-point between transits. Since the eclipse duration is ∼1-hour, the sensitivity of the eclipse time to moderately small eccentricity ($e = 0.15$ for GJ 436b) is obvious.

2.1. *Molecular Absorption*

The actual flux from close-in planets will peak near 2 to 5 μm, not at the wavelengths of greatest contrast. Moreover, the shorter infrared (IR) wavelengths are key to inferring the composition and temperature structure of the planet's atmosphere. Figure 3 shows the spectrum of HD 189733b, in flux (not contrast) units, from Barman (2008). The IR spectra of hot Jupiters are believed to be shaped predominantly by water absorption (Burrows *et al.* 2005, Seager *et al.* 2005), but other molecules such as methane also play a role (e.g., Swain *et al.* 2008a), and methane in particular could become more important for cooler planets like GJ 436b. For close-in planets orbiting luminous stars, strong irradiation could flatten the temperature gradient and weaken absorption features in the spectrum at the time of eclipse (Fortney *et al.* 2006). *Spitzer* results from spectroscopy initially suggested that water absorption might not be a prominent feature in eclipse spectra (Grillmair *et al.* 2007, Richardson *et al.* 2007, see discussion below). However, the HD 189733b results from IRAC (Charbonneau *et al.* 2008) are in good accord with Barman's standard model, and provide convincing evidence that water absorption shapes the 2- to 5 μm spectra of at least one hot Jupiter.

Important observations of *transits* have also been made using *Spitzer* (Richardson *et al.* 2006, Gillon *et al.* 2007, Nutzman *et al.* 2008, Agol *et al.* 2008), including evidence for water absorption during transit (Tinetti *et al.* 2007, Beaulieu *et al.* 2008). Ehrenreich *et al.* (2007) have suggested that better correction for instrument systematics is needed before we can conclude that water absorption is detected via IRAC photometry during transit. While I believe there is good evidence for water absorption in transit, additional work to better understand *Spitzer's* instrumental systematics is certainly warranted.

2.2. *Circulation and Dynamics*

Hot Jupiters are believed to rotate synchronously with their orbital period, keeping one side perpetually pointed toward the star. An important question is the degree to which they transport heat to the anti-stellar hemisphere via strong atmospheric circulation. Models of this circulation (e.g., Showman & Guillot 2002, Cho *et al.* 2003, 2008, Cooper and Showman 2006, Langton and Laughlin 2008) can be checked using *Spitzer* around-the-orbit observations, either made continuously (Knutson *et al.* 2007), or via periodic sampling (Harrington *et al.* 2006, Cowan *et al.* 2007). Observations of two non-transiting hot Jupiters, Ups And b at 24 μm (Harrington *et al.* 2006) and HD 179949b at 8 μm (Cowan *et al.* 2007) suggested large day-to-night temperature contrasts. Other planets

https://doi.org/10.1017/S1743921308026410 Published online by Cambridge University Press

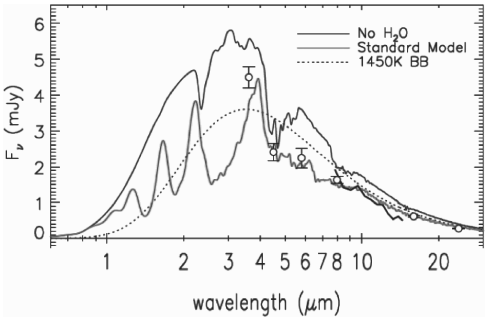

Figure 3. Modeled spectrum of HD 189733b, giving flux vs. wavelength in microns, from Barman (2008), with measurements from Charbonneau *et al.* (2008). The standard model including water absorption provides the best fit to the measurements.

give much lower day-night contrast (Knutson *et al.* 2007, Cowan *et al.* 2007). One possibility is that the difference for Ups And b is related to the greater formation height of 24 μm radiation. But note that Knutson *et al.* (2008a) have observed HD 189733b at 24 μm, and find a result commensurate with their 8 μm results. Another possibility is that these type of phased observations could be affected by a temporary 'hot spot', and would not typically show such a large day-night difference. However, in that case we would also expect greater-than-predicted variability at secondary eclipse for some transiting planets, and even low-level variability has not yet been observed. *Spitzer* will re-observe Ups And b at 24 μm (B. Hansen, private communication) if the cryogen lasts long enough.

In addition to close-in planets on circular orbits, *Spitzer* has great potential to observe the time-dependent heating (Iro & Deming 2008) for planets on very elliptic orbits. Recently, Laughlin *et al.* (2008) observed the flash-heating of HD 80606b at periastron, and *Spitzer* may be able to make more observations of this type during the warm mission.

2.3. *Inverted Temperature Gradients*

Although HD 189733b shows water absorption, and agrees well with standard models, there is evidence that other exoplanets show different atmospheric structures. HD 209458b exhibits an atmospheric temperature inversion (i.e., temperature rises with increasing height). The first hint of this inversion was found by Richardson *et al.* (2007), who derived emission features in their eclipse spectrum at relatively 'high' spectral resolution $\lambda/\delta\lambda \sim 100$, albeit at low signal-to-noise. Definitive evidence of the inversion comes from the IRAC eclipse measurements by Knutson *et al.* (2008b). Figure 4 shows the IRAC measurements for both HD 189733b (Charbonneau *et al.* 2008, Barman 2008) and HD 209458b (Knutson *et al.* 2008b, Burrows *et al.* 2007), compared with models from Burrows *et al.* (2008). In comparing the observations and models on Figure 4, I have scaled the models by an arbitrary contrast factor to produce the best fit by eye. This serves to illustrate the nature of these two different exoplanet spectra, but I caution that for the quantitative fits, readers should consult the original papers.

In addition to IRAC, *Spitzer* eclipse observations of both planets have been obtained at 16 μm and 24 μm (not plotted). These longer wavelengths are also sensitive to water absorption and atmospheric temperature gradients, but less so than at IRAC wavelengths. When comparing spectral energy distributions for different planets, remember that all four IRAC wavelengths were observed simultaneously only for HD 189733b and HD 209458b. More commonly, due to the nature of the instrument (Fazio *et al.* 2005), eclipses are measured at 3.6 and 5.8 μm simultaneously, and then in another eclipse at 4.5 and 8 μm simultaneously. In principle, variability of the planet's thermal emission

https://doi.org/10.1017/S1743921308026410 Published online by Cambridge University Press

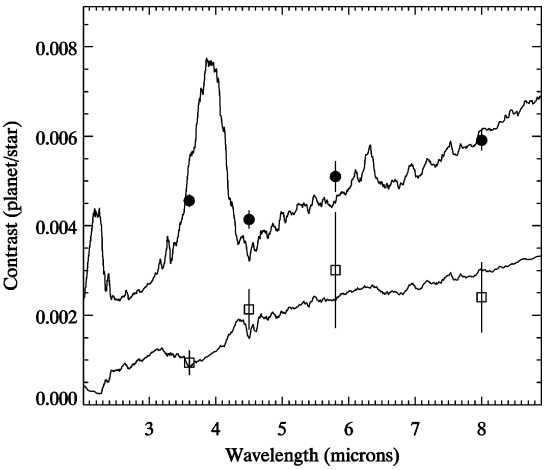

Figure 4. Measurements of HD 189733b from Charbonneau *et al.* (2008), and HD 209458b from Knutson *et al.* (2008b), compared to a standard model (HD 189733b) and a temperature-inverted model (HD 209458b) from Burrows *et al.* (2008). The model and observations for HD 189733b have been offset upward by 0.002 for clarity. Error bars are $\pm 2\sigma$.

(Rauscher *et al.* 2007) could contaminate the measured spectrum. To date, there is no evidence for variability large enough to produce significant spectrum errors (see Agol *et al.* 2008).

The hallmark of an inverted spectrum can be seen by comparing 5.8 and 8.0 μm measurements, as well as comparing 3.6 and 4.5 μm. The inverted atmosphere has a higher 5.8 μm flux than 8.0 μm, because 5.8 μm has high opacity due to water vapor, and the water bands are present in emission. In the non-inverted atmosphere the 3.6 μm flux is elevated because the lesser opacity at this wavelength allows planet flux to well up from the deeper atmosphere, where temperatures are higher. The non-inverted 4.5 μm band shows lower flux because water and CO opacity cause the radiation to be emitted from higher layers of the atmosphere, where the temperature is lower. The inverted atmosphere may have a high altitude absorbing layer (Burrows *et al.* 2008), and this raises the temperature at the 4.5 μm height, and lowers it at the 3.6 μm height, reversing the relative magnitudes of the emergent fluxes.

An open question is the physical cause of the inversion, and whether this is a common phenomenon in hot Jupiter atmospheres. Burrows *et al.* (2008) attribute the inversion to the presence of a high altitude optical absorbing layer, but the composition and origin of this layer are unknown. Doubtlessly, the high level of stellar irradiation that hot Jupiters experience plays a major role in inverting the temperature gradient. Fortney *et al.* (2008) define two classes of hot Jupiters depending on whether the stellar irradiation drives the formation of a hot stratosphere (i.e., region of higher temperature) via TiO/VO absorption. TiO and VO have bands in the optical where stellar fluxes are high, and have been implicated in perturbations to exoplanet atmospheric temperature structure (Hubeny *et al.* 2003). Figure 5 shows many of the known exoplanets in mass vs. irradiance space, with the predicted boundary between the pM class (stratospheres) and pL class (no stratospheres) indicated. I have circled the three planets that are known or strongly suspected to have inverted temperature gradients. Besides HD 209458b, HD 149026b is believed to have a hot stratosphere on the basis of the very high brightness temperature at 8 μm (Harrington *et al.* 2007). Recently, XO-1b was found to have an inverted gradient (Machalek *et al.* 2008). Although XO-1b is predicted to be pL class, it is at the upper

https://doi.org/10.1017/S1743921308026410 Published online by Cambridge University Press

range of that class, so there is no firm counterexample to the Fortney *et al.* (2008) theory at this point. In the present volume, new information is presented on TrES-2 (O'Donovan *et al.*) and TrES-4 (Knutson *et al.*), and *Spitzer* data for several other planets are under analysis. Hence we should soon learn how well the curent pM/pL classification theory corresponds to reality.

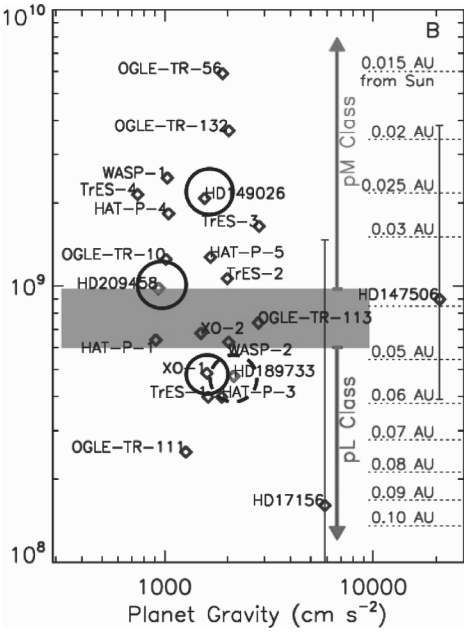

Figure 5. Atmospheric structure classification for hot Jupiters, from Fortney *et al.* (2008). The pM class planets are predicted to have hot stratospheres (i.e., temperature inversions), whereas the pL class planets should not. The planets that are currently known or strongly suspected to have inversions are circled with solid lines, and the non-inverted planets (TrES-1, and HD 189733b) are circled with dashed lines.

2.4. *A Hot Neptune*

Spitzer secondary eclipse observations extend down to the hot Neptune orbiting GJ 436 (Deming *et al.* 2007a, Demory *et al.* 2007). Figure 6 shows this eclipse at 8 μm. The inferred brightness temperature (712 ± 36K) is modestly above the predicted brightness temperature for thermal equilibrium with the star (Deming *et al.* 2007a), but the uncertainties are relatively large. Additional *Spitzer* eclipse observations were recently made at 8- and 24 μm (J. Harrington, private communication) and 'around-the-orbit' observations (by Knutson *et al.*) are pending. The totality of *Spitzer* observations may be sufficient to define the total luminosity of the planet, and thereby determine whether it emits significant energy due to tidal dissipation in its moderately eccentric orbit.

3. Spectroscopy

Spitzer secondary eclipse observations have been extended to spectroscopy as well as photometry (Grillmair *et al.* 2007, Richardson *et al.* 2007, Swain *et al.* 2008b). The principle of these measurements is simple. Suppose that an absorption (emission) feature occurs in the planets atmosphere at a given wavelength. Then the depth of the eclipse at that wavelength will be smaller (larger) than at other wavelengths. Hence the emergent

https://doi.org/10.1017/S1743921308026410 Published online by Cambridge University Press

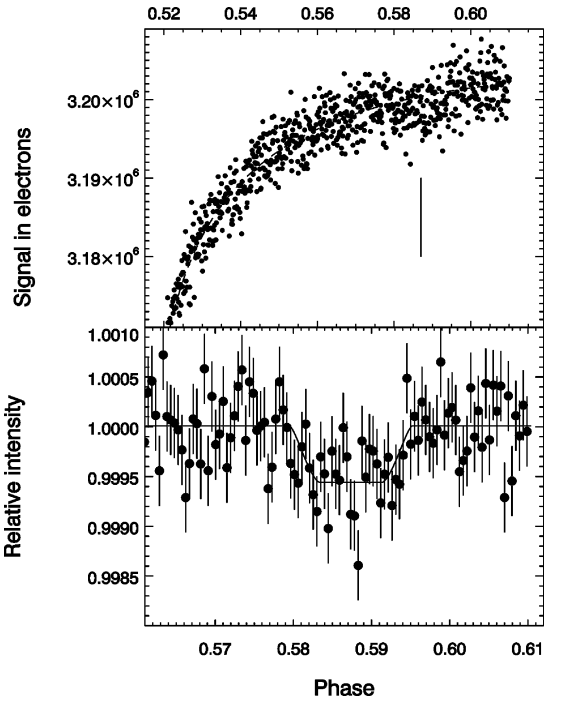

Figure 6. Secondary eclipse of the hot Neptune planet GJ 436b observed by *Spitzer* at 8 μm (Deming *et al.* 2007a). The top panel shows the unbinned data prior to correction of the detector ramp, and the lower panel shows binned data and a fit of an eclipse curve centered at phase 0.587, indicative of an eccentric orbit.

spectrum of the planet can be constructed from the wavelength dependence of the eclipse depth. In practice, this is a much more difficult observation than *Spitzer* photometry, for two reasons. First, there are many fewer photons per wavelength channel because the light is dispersed, so the signal-to-noise ratio is lower than for photometry. Second, spectroscopy is more affected by instrument systematic effects, as discussed below. In spite of these difficulties, the results are of great interest. Two exoplanets are sufficiently bright to make *Spitzer* spectroscopy practical: HD 189733b (Grillmair *et al.* 2007), and HD 209458b (Richardson *et al.* 2007, Swain *et al.* 2008b). The initial results indicated that these spectra were remarkably flat from ~ 7 to $\sim 13\,\mu$m, not showing absorption due to water vapor that was expected shortward of $\sim 8\,\mu$m. However, additional spectroscopy of HD 189733b (Grillmair, private communication) agrees very well with *Spitzer* photometry and with model atmosphere predictions. HD 209468b having an inverted temperature gradient is consistent with the flatness observed in the spectrum by Richardson *et al.* (2007).

Grillmair *et al.* (2007) did not find evidence for discrete spectral absorption/emission features in the spectrum of HD 189733b, but Richardson *et al.* (2007) concluded that the spectrum of HD 209458b contained two discrete features, both present in emission. Near 9.8 μm they found evidence for a relatively broad emission bump that they attributed to the Si-O stretching resonance, and at 7.78 μm they find a sharp emission feature that may be due to a C-C stretching resonance. To illustrate these results, I have re-analyzed the Richardson *et al.* data, using a similar method, and this result is shown in Figure 7. These data have also been analyzed by Swain *et al.* (2008b), using an entirely different method. Swain *et al.* find emission near 7.8 μm, but not at 9.8 μm. This difference in

https://doi.org/10.1017/S1743921308026410 Published online by Cambridge University Press

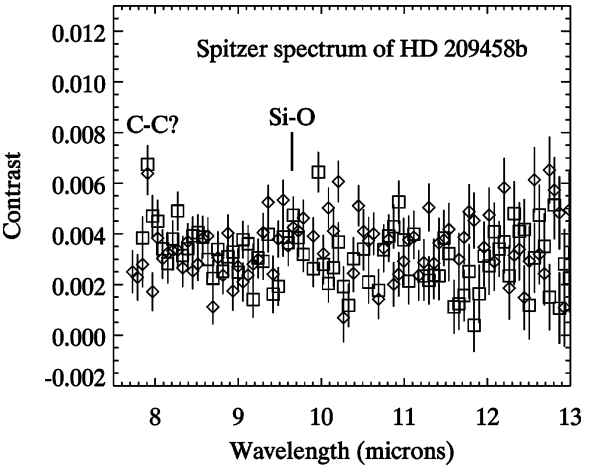

Figure 7. Spectrum of HD 209458b, derived using an analysis very similar to Richardson *et al.* (2007), based on two eclipses (different symbols). The two emission features evident in the spectrum are a broad bump near 9.8 μm that Richardson *et al.* attribute to silicate clouds, and a sharp emission feature at 7.78 μm possibly due to a C-C stretching resonance.

results seems consistent with the nature of the systematic effects in the IRS instrument: broad features (9.8 μm) are more sensitive to the way the instrument systematics are treated in the analysis, whereas sharp features (7.8 μm) are insensitive to the analysis method. It is important to optimize the spectroscopic eclipse technique, so that we can use it with JWST to measure the spectra of potentially habitable planets transiting M-dwarfs (Charbonneau and Deming, 2007).

4. *Spitzer* Instrument Systematics

Spitzer observations have proven to be a remarkably stable and sensitive way to measure exoplanet thermal emission. *Spitzer* exoplanet aperture photometry (for $\lambda \leqslant 8\,\mu$m) achieves noise levels closely approaching the photon noise limit, and the errors average down as the inverse square root of exposure time. For the longer *Spitzer* wavelengths, where the zodiacal thermal background is significant, the most precise photometry often requires PSF-weighted optimal photometry, depending on the brightness of the star. Unlike ground-based photometry, it is generally *not* necessary to use 'comparison stars' with *Spitzer*. In fact, it can even be detrimental to rely on comparison stars, because *Spitzer* does have instrument systematic effects that could vary with position on the detector. There are several effects that are currently recognized and accounted for in *Spitzer* analyses, and most of them are now described in the *Spitzer* instrument documentation. The ones most relevant to exoplanet eclipses are:

The Ramp. Photometry at 8- and 16 μm exhibits a gradually increasing intensity, equivalent to an increasing gain in the instrument response. This apparent gain increase is flux-dependent: bright sources reach maxmium intensity more rapidly than faint sources. This so-called 'ramp' (Deming *et al.* 2006) is obvious in the top panel of Figure 6. Knutson *et al.* (2007) hypothesize that it is due to charge-trapping, which is (so far) the most promising hypothesis. Note that the ramp is *not* simply due to build-up of a latent image, since none is present when the telescope is nodded (Deming *et al.* 2006). In the charge-trapping hypothesis, the first electrons generated by photons are captured by ionized impurites in the detector material, and do not contribute to the signal on

https://doi.org/10.1017/S1743921308026410 Published online by Cambridge University Press

the observed time scale. As the detector is exposed to additional radiation, the charge traps saturate, and the signal readout reaches an asymptotic level. This explanation is broadly consistent with the known characteristics of the ramp, with some exceptions. Observations at 5.8 μm can exhibit a 'negative' ramp, i.e. a decreasing intensity with time (Machalek *et al.* 2008), and no ramp is seen in 24 μm photometry (Knutson and Charbonneau, private communication). The existence of decreasing, as well as increasing, ramps suggests a complex phenomenon that may depend on the gate and bias voltages applied to the detector. The lack of a ramp at 24 μm may be due to the fact that the relatively large zodiacal background at this wavelength keeps the ramp perpetually at its maximum value, but the zodiacal background is also strong for 16 μm photometry, which does exhibit a prominent ramp (Deming *et al.* 2006). Spectroscopy using IRS also exhibits a ramp, at least when obtaining spectroscopy at 7-14 μm (Richardson *et al.* 2007).

The ramp is a relatively benign effect for eclipse photometry of bright and high-contrast systems. The time scale for the ramp to reach its maximum value is significantly longer than the duration of an eclipse, so it's essentially a baseline effect that is included when fitting to the eclipse depth. But the ramp is more problematic for fainter and low-contrast systems because small uncertainties in the ramp curvature become significant relative to the eclipse depth. The ramp is also problematic for 'around-the-orbit' observations where the planet signal will vary on a longer time scale. One promising approach for this type of observation is to 'pre-flash' the detector by exposing it to a bright source immediately prior to the exoplanet observations. This saturates the ramp before the exoplanet is observed; preliminary examination of observations using a pre-flash (H. Knutson, private communication) suggest that the technique is largely successful.

Pixel Phase. The pixels in the IRAC detectors are more responsive when stellar images are centered on the pixels than when they lie near the edges, and this is called the pixel phase effect. One exception to this is very bright stars that are near saturation. Detector non-linearity can produce a lower signal when very bright stars are centered on a given pixel, but this circumstance is normally avoided by using shorter integration times. The pixel phase effect is ubiquitous in the 3.6 and 4.5 μm channels of IRAC, and may be present to a much lesser degree at 5.8- and 8 μm. Because there is pointing jitter in the telescope ($\sim$ tens of milli-arcsec), the pixel phase effect leads to a variable intensity when performing aperture photometry. This is corrected in eclipse data by decorrelating the intensity versus distance from pixel center (e.g., Charbonneau *et al.* 2005, 2008). Pixel phase is also normally decorrelated from photometry performed for other *Spitzer* research (Morales-Calderon *et al.* 2006), not just exoplanet photometry.

Spectroscopic Slit Losses. The IRS spectrometer (Houck *et al.* 2005) has light losses at its entrance slit, like most astronomical slit spectrometers. Diffraction causes stellar images at the slit to increase in size proportional to wavelength, so the slit losses increase with wavelength also. Because there is telescope pointing jitter on a time scale of $\sim$ 1 hour, and possibly on longer times scales, the intensity in a stellar spectrum will vary slightly with both wavelength and time. Even a slight variation in the measured stellar spectrum distorts the spectra that are inferred for exoplanets using the eclipse technique. There is no robust and independent method to ascertain the exact telescope pointing for a given spectrum. Hence exoplanet observers correct for this distortion in different ways (Richardson *et al.* 2007, Swain *et al.* 2008b). Because the effect varies slowly with wavelength, it primarily affects broad features in exoplanet spectra, not sharp features like the 7.8 μm emission inferred in HD 209458b (Richardson *et al.* 2007, and Figure 7). Hence the appearance of broad features (like the 9.8 μm peak on Figure 7), and indeed their reality in exoplanet spectra, can depend on the method used to analyze the data.

https://doi.org/10.1017/S1743921308026410 Published online by Cambridge University Press

Sharp features should be robust against instrument systematics, but I note that the 7.8 μm feature has relatively low signal-to-noise.

5. Warm Spitzer

The depletion of cryogen (in $\sim$ April 2009) will terminate the cold portion of the *Spitzer* mission. However, the 3.6 and 4.5 μm channels of IRAC will still operate at full sensitivity, because the observatory will remain radiatively cooled at $\sim$ 35K. The requirement to operate the 'warm' mission at low cost dictates that operations must be simple. This favors relatively large programs, and exoplanet transit and eclipse science is poised to take full advantage of *Warm Spitzer*. A 'not-yet-obsolete' discussion of some possible exoplanet applications is given in Deming *et al.* (2007b).

6. Tabular Summary of the Spitzer Results

The legacy of exoplanet science from cryogenic *Spitzer* has already revolutionized exoplanet science, but has not yet reached full fruition. The results are of uniformly high quality, but the observations are not easy. The table in Figure 8 summarizes my personal opinion as to which of the *Spitzer* results are already robust, and which aspects need clarification by additional work.

Robust Now	***Needs More Work***
Broadband Spectra for High-contrast Systems (e.g. 189733b, 209458b) **Inverted temperature gradients exist**	**Broadband spectra for lower contrast and fainter systems (ramp shape is significant to eclipse depth, e.g. 149026b)** **Inversions for weakly irradiated planets?** **Variability of eclipse depth**
Water absorption on 189733b day side	**Water absorption during transit (increased accuracy at 3.6 & 4.5 microns)**
Longitudinal temperature for 189733b (have two wavelengths, in agreement)	**Around-the-orbit observations on other systems - need to flatten the ramp** **Need more Ups And measurements**
Sharp features in IRS spectra (7.8-micron)	**Broad features in IRS spectra**
Flash-heating in eccentric orbits	**Flash-heating in eccentric orbits**

Figure 8. Tabular summary of the Spitzer results, categorized by results that are already robust, and those where more work is needed. Observations of eccentric planets fall into both categories, because the current work should be extended to more planets.

Acknowledgements. Adam Burrows, Travis Barman, Dave Charbonneau, Jonathan Fortney, Heather Knutson, and Francis O'Donovan all made valuable comments on a draft of this review. I thank Travis and Jonathan for providing Figures 3 and 5.

References

Agol, E., Cowan, N. B., Bushong, J. *et al.* 2008, *this volume*.
Barman, T. 2008, *ApJ*, 676, L61.
Beaulieu, J. P., Carey, S., Ribas, I., *et al.* 2008, *ApJ* 677, 1343.
Bouchy, F., Udry, S., Mayor, M., *et al.* 2005, *A&A* 444, L15.
Burrows, A., Hubeny, I., & Sudarsky, D. 2005, *ApJ* 625, L135.
Burrows, A., Hubeny, I., Budaj, J., Knutson, H. A., & Charbonneau, D. 2007, *ApJ*, 668, L171.
Burrows, A., Hubeny, I., Budaj, J., *et al.* 2008, *ApJ*, 668, L171.
Charbonneau, D. 2003, *A. S. P. Conf. Ser.*, 294, 449.
Charbonneau, D., Allen, L. E., Megeath, S. T., *et al.* 2005, *ApJ* 626, 523.
Charbonneau, D. & Deming, D. 2007, astro-ph/0706.1047.
Charbonneau, D., Knutson, H. A., Barman, T., *et al.* 2008, *ApJ*, in press, astro-ph/0802.0845.
Cho, J. Y.-T., Menou, K., Hansen, B., *et al.* 2003, *ApJ*, 587, L117.
Cho, J. Y.-T., Menou, K., Hansen, B., *et al.* 2008, *ApJ*, 675, 817.
Cooper, C. S. & Showman, A. P. 2005, *ApJ*, 629, L45.
Cowan, N. B., Agol, E., & Charbonneau, D. 2007, *Mon. Not. Roy. Astr. Soc.*, 379, 641.
Deming, D., Seager, S., Richardson, L. J., *et al.* 2005, *Nature* 434, 740.
Deming, D., Harrington, J., Seager, S., *et al.* 2006, *ApJ* 644, 560.
Deming, D., Harrington, J., Laughlin, G., *et al.* 2007a, *ApJ* 667, L199.
Deming, D., Agol, E., Charbonneau, D., *et al.* 2007b, *AIP Conf. Proc.* 943, 89, astro-ph/0710.4145.
Demory, B.-O., Gillon, M., Barman, T., *et al.* 2007, *A&A*, 475, 1125.
Ehrenreich, D., Hebrard, G., Lecvelier des Estangs, A., *et al.* 2007, *ApJ*, 668, L179.
Fazio, G. G., Hora, J. L., Allen, L. E., *et al* 2004, *ApJ Suppl.* 154, 10.
Fortney, J. J., Cooper, C. S., Showman, A. P., *et al.* 2006, *ApJ*, 652, 746.
Fortney, J. J., Lodders, K., Marley, M. S., *et al.* 2008, *ApJ*, 678, 1419.
Gillon, M., Demory, B.-O., Barman, T., *et al.* 2007, *A&A* 471, L51.
Grillmair, C. J., Charbonneau, D., Burrows, A., *et al.* 2007, *ApJ* 658, L115.
Harrington, J., Hansen, B. M., Lusczc, S. H., *et al.* 2006, *Science*, 314, 623.
Harrington, J., Luszcz, S., Seager, S., *et al.* 2007, *Nature*, 447, 691.
Houck, J. R., Roellig, T. L., van Cleve, J., *et al.* 2004, *ApJ Suppl.* 154, 18.
Hubeny, I., Burrows, A., & Sudarsky, D. 2003, *ApJ*, 594, 1011.
Iro, N. & Deming, D. 2008, *this volume*, astro-ph/0807.0266.
Knutson, H. A., Charbonneau, D., Allen, L. E., *et al.* 2007, *Nature*, 447, 183.
Knutson, H. A., Charbonneau, D., Cowan, N. B., *et al.* 2008a, *ApJ, submitted*, astro-ph/0802.1705.
Knutson, H. A., Charbonneau, D., Allen, L. E., *et al.* 2008b, *ApJ*, 673, 526.
Langton, J. & Laughlin, G. 2008, *ApJ*, 674, 1106.
Laughlin, G., Deming, D., Langton, G. 2008, *Nature*, submitted.
Machalek, P., McCullough, P., Burke, C. J., *et al.* 2008, *ApJ*, in press, astro-ph/0805.2418.
Morales-Calderon, M., Stauffer, J. R., Kirkpatrick, J. D., *et al.* 2006, *ApJ*, 653, 1454.
Nutzman, P., Charbonneau, D., Winn, J. N., *et al.* 2008, *ApJ*, submitted, astro-ph/0807.1318.
Rauscher, E., Menou, K., Cho, J. Y.-K., *et al.* 2007, *ApJ*, 662, L115.
Richardson, L. J., Harrington, J., Seager, S., *et al.* 2006, *ApJ*, 649, 1043.
Richardson, L. J., Deming, D., Horning, K., *et al.* 2007, *Nature*, 445, 892.
Seager, S., Richardson, L. J., Hansen, B. M. S., *et al.* 2005, *ApJ*, 632, 1122.
Showman, A. P. & Guillot, T. 2002, *A&A*, 385, 166.
Swain, M. R., Gautam, V., & Tinetti, G. 2008a, *Nature*, 452, 329.
Swain, M. R., Bouwman, J., Akeson, R. L., *et al.* 2008b, *ApJ*, 674, 482.
Tinetti, G., Vidal-Madjar, A., Liang, M.-C., *et al.* 2007, *Nature*, 448, 169.